Electron traps and scintillation mechanism in $LuAlO_3$:Ce

2001 J. Phys.: Condens. Matter 13 9599

(http://iopscience.iop.org/0953-8984/13/42/318)

INSTITUTE OF PHYSICS PUBLISHING JOURNAL OF PHYSICS: CONDENSED MATTER

J. Phys.: Condens. Matter **13** (2001) 9599–9619 PII: S0953-8984(01)23873-9

Electron traps and scintillation mechanism in $LuAlO_3$:Ce

Andrzej J Wojtowicz[1], Piotr Szupryczynski[1,2], Dariusz Wisniewski[1], Jaroslaw Glodo[1] and Winicjusz Drozdowski[1]

[1] Laboratory of Solid State Optoelectronics, Institute of Physics, N Copernicus University, Grudziadzka 5/7, PL 87-100 Torun, Poland
[2] Chemistry Department, Boston University, 590 Commonwealth Avenue, Boston, MA 02215, USA

E-mail: andywojt@phys.uni.torun.pl

Received 11 April 2001, in final form 4 July 2001
Published 5 October 2001
Online at stacks.iop.org/JPhysCM/13/9599

Abstract

In this paper we report measurements of thermoluminescence in the temperature range of 20–370 K, isothermal decays, pulsed vacuum ultraviolet and γ-excited luminescence time profiles at various temperatures on cerium-activated orthoaluminate ($LuAlO_3$:Ce, LuAP), a new and promising scintillator material. We demonstrate that results of all these experiments can be consistently explained by assuming a recombination mechanism of scintillation light production in the LuAP scintillator. Using a simple first-order kinetic model that includes Ce^{3+} ions as recombination centres and a number of electron traps, we extract from experimental data the basic trap parameters (energy depths and frequency factors). Consequently we identify nine traps that are responsible for undesired features of the LuAP scintillator, such as a reduced scintillation light output, a relatively long scintillation rise time and slow scintillation components (afterglow) at room temperature. We demonstrate that some of these traps are responsible for large variations of the scintillation light yield with temperature as reported earlier. Although the deepest traps do not alter scintillation time profiles, they are responsible for a significant scintillation light loss and are, therefore, detrimental to scintillation performance of the material. We observe that there is an apparent correlation between trap depths and frequency factors for at least five of the traps that may fit some more general pattern involving various groupings of all the traps. This, in turn, would indicate that traps in LuAP are not unrelated and are due, most likely, to a series of native defects in the LuAP crystal structure. Although the specific identity of traps remains unknown, the performance of the LuAP scintillator is now, in practical terms, fully understood and can be described numerically at any temperature using a model and a set of parameters given in this paper. It is clear that any major improvement of the material would require

that traps are eliminated or that their influence on the scintillation process is minimized.

1. Introduction

Wide-bandgap materials have long been the subject of active research as scintillator detectors of ionizing radiation in high energy and nuclear physics (detectors), in industry (quality control, oil exploration and airport security) and in medicine (γ-ray detectors for positron emission tomography (PET) and computed tomography (CT)). A number of materials, such as NaI:Tl, CsI:Tl, CaF_2:Eu and BGO ($Bi_4Ge_3O_{12}$), have a long history of use in these applications. Although the exceptionally high density of BGO (7.13 g cm^{-3} against 3–5 g cm^{-3} for halides) promoted its use in the world's largest crystal calorimeter L3 at the LEP collider in CERN [1] and in PET machines [2], its relatively low efficiency (light yield (LY) of only 8000 photons M eV^{-1}) and slow scintillation decay (about 360 ns) fall short of requirements of modern applications.

The stringent density, efficiency and timing requirements of modern applications became a driving force behind a worldwide search for new scintillator materials that was initiated in the late 1980s. These efforts led to the discovery of a number of promising new materials, characterized by reasonably high density, high LY and fast decay and rise times. The most prominent of these, and the most developed, is LSO (Lu_2SiO_5:Ce), discovered by Melcher and Schweitzer in 1992 [3]. Another material with attractive properties, but far less advanced in development, is LuAP ($LuAlO_3$:Ce), suggested as a scintillator material by Baryshevsky *et al* [4] and Minkov [5], and evaluated in a powder and garnet contaminated forms by Moses *et al* [6]. Czochralski-grown garnet-free perovskite phase monocrystals of LuAP (Litton Airtron) were first evaluated by Lempicki and collaborators in 1994 [7] and then by Moszynski *et al* [8]. Crystals grown by both Czochralski (Preciosa) [9] and Bridgman (Armenian National Academy of Sciences) [10] have been extensively studied in the frame of the Crystal Clear Collaboration since 1995 [11–14].

The advantages of the vacuum ultraviolet (VUV) studies on scintillator materials have been demonstrated in numerous publications [15]. While radioluminescence spectra excited by gamma or x-radiation invariably reflect the dominant radiative decay mode of the relevant electronic excitations of the material (electron–hole pairs and/or excitons), photoluminescence spectra often show a strong dependence upon the wavelength of excited light, indicating the existence of competing energy transfer channels to various emitting centres. The VUV excitation spectra of the 'host' and Ce emissions in 'undoped' and Ce-doped LuAP in the vicinity of the bandgap energy have led Wojtowicz [16] and then Wisniewski *et al* [17] to propose that the dominant mechanism of scintillation light production in this material is due to consecutive capture of electron–hole pairs and not excitons. Pedrini *et al* reached to similar conclusions based on a qualitative analysis of x-ray photoelectron spectroscopic results on oxides and fluorides [18]. Using a simple single-configuration-coordinate model, Wojtowicz *et al* [19] demonstrated that sequential trapping of charge carriers involving different Ce charge states is a likely mechanism of the host-to-ion energy transfer in LuAP and that a sequence of the capture processes is initiated by a hole capture (creating Ce^{4+}).

Thermoluminescence (TL) has proved to be a useful tool for studies of lattice defects and carrier traps in wide-bandgap materials [20]. Early TL studies of LuAP at 300–700 K [21, 22] provided evidence that recombination of charge carriers via Ce^{3+} is the dominant mechanism by which scintillation light is produced in this material and established

parameters of a number of deep traps responsible for TL glow peaks between 300 and 700 K. Bartram *et al* [23] measured the scintillation light loss due to these deep traps by directly comparing the TL released during the heating of the sample between 34 and 290 °C and integrated radioluminescence output during the preceding steady-state γ-irradiation in the same cycle. Unfortunately the measured ratio is severely underestimated since the contribution of relatively fast components due to shallow traps, and responsible for decrease in the time-gated scintillation LY, cannot be properly estimated from such an experiment. Strong variations of the steady-state radioluminescence intensity on the timescale of 10 ms, 1 and 200 s as well as large differences between time-gated and steady-state LYs have indeed been observed by Dujardin *et al* [13, 14] and ascribed to traps.

By using an approximate formula expressing the time-gated scintillation LY in terms of trap parameters, Ce^{3+} radiative lifetime, branching coefficients and temperature (instantaneous or zero-time amplitude approximation), Wojtowicz *et al* [24] analysed a step-like increase of the scintillation LY in LuAP between 300 and 400 K. They demonstrated that the apparent correlation with the trap glowing at 340 K is misleading and that this step in the yield curve is actually due to a much shallower trap that presumably has its glow peak in the range of 150–180 K. More detailed studies of thermal dependence of the scintillation LY in LuAP revealed that there must be a second, even shallower, trap responsible for an additional step between 120 and 170 K as well as for a relatively slow rise time (0.6 ns) in the scintillation time profile of LuAP [25]. The hypothetical glow curve due to this second trap was estimated to peak at about 75 K [26]. All these results suggested that TL experiments at lower temperatures, say, between 20 and 300 K, might reveal other, at that time unknown, glow peaks.

Such experiments have been performed at Boston University and initial results, obtained after the VUV irradiation, have already been published [27, 28]. The glow curves do show, as expected, a number of TL glow peaks at lower temperatures, quantitative analysis of which yielded the corresponding trap depths and frequency factors. However, these results, based exclusively on the analysis by Randall and Wilkins of the TL glow peaks [29], are not entirely reliable and have not been used to establish a link between traps and scintillation characteristics of a given material including steps in the yield–T curve as well as the particular components in the scintillation time profiles. Only recently traps and their parameters have been derived from the low-temperature TL experiments following the VUV irradiation being quantitatively correlated with the basic scintillation characteristics of LuAP:Ce and YAP:Ce ($YAlO_3$:Ce, Y-based perovskite aluminate analogue of LuAP) [30].

Phosphorescence isothermal decays (ITDs) [20] have been demonstrated to provide a useful supplement of the TL glow curve measurements that help to uncover smaller, hidden glow peaks [25]. ID time constants have also been found very helpful in constructing the Arrhenius type diagrams used to extract trap parameters and identify traps responsible for various components in the scintillation time profiles of BaF_2:Ce [31].

Scintillation time profiles of γ-excited LuAP at temperatures between 35 and 580 K were measured and reported earlier [27]. Unfortunately time constants and contributions of various observed scintillation decay components did not appear to follow any apparent trends, and consistent interpretation of these results is still lacking.

In their report Wojtowicz *et al* [32] noted the peculiar difference in time profiles of Ce emission in LuAP excited by synchrotron pulses of different wavelengths. They observed that direct excitation into any of the Ce^{3+} ion absorption bands produces nearly single-exponential decays of about 17 ns and of only very short rise times, most likely reflecting the instrumental response function. In contrast, all the profiles obtained for excitation at shorter wavelengths contain components that, depending on temperature, are significantly slower and clearly display some finite rise times. The Arrhenius plot of rise time constants against inverse

temperature yielded parameters that were reasonably close to trap parameters obtained from the fit to the scintillation yield dependence on temperature [25], supporting the notion of the recombination mechanism of the light production in LuAP that involves electron traps.

Consequently it has been suggested that results of all the experiments on LuAP and YAP, such as TL (at and above 300 K), low-temperature TL (ltTL, 20–370 K), scintillation LY against temperature (LY against T) and scintillation time profiles (STPs) at various temperatures can be consistently interpreted in the frame of a simple model that includes one recombination centre (Ce^{3+}) and a number of electron traps acting under first-order kinetics [24–26, 32, 33]. The model successfully explains the observed peculiar differences between Lu- and Y-based perovskite scintillators [26]. The more rigorous treatment has also been advanced by Lempicki and Bartram [34]. In their treatment the more general second-order kinetics is simplified to first-order, allowing an analytical solution. Alternatively the second-order equations are solved numerically. Both approaches correctly predict some features displayed by the LY–T curves in LuAP and YAP but complications render the involved fitting procedure impractical in the case of two and more traps.

In this paper we supplement the initial and partially published experimental results on LuAP presented above. We report improved measurements of the ltTL following the x-ray (not VUV) irradiation that reveal new glow peaks at temperatures between 20 and 370 K, new measurements of the ITDs in the vicinity of all known and new glow peaks between 20 and 370 K and, finally, the emission time profiles under pulsed synchrotron excitation in the VUV spectral range at various temperatures. All these results as well as previously obtained scintillation time profiles under γ-excitation are then used in order to extract trap parameters by means of an Arrhenius diagram showing all the measured time constants against inverse temperature.

We find that the scintillation process in γ-excited LuAP can be consistently described by means of the recombination model consisting of Ce^{3+} recombination centres and a range of electron traps, and evolving under first-order kinetics.

2. Crystals and experimental set-ups

The samples of LuAP were cut from the two boules provided by M Randles (Synoptics Division, Litton-Airtron Corp, Charlotte, NC). The crystals were pulled from the melt (Czochralski method) on an iridium wire in an atmosphere of N_2. The Ce concentrations in the melt were 0.25 and 0.75 mol% but the actual concentrations found by mass spectroscopy analysis were only 200 and 600 ppmw.

The ltTL glow curves were measured using a closed-cycle double compressor He cooler with a programmable temperature controller. Prior to TL runs the samples were irradiated for about 18 h by an x-ray source (Cd^{109}) at 4 K. During TL runs the heating rate was kept constant at 9 K min^{-1}. The ITD experiments were performed using the same set-up but with a different heating cycle; the sample was irradiated at 4 K and then the temperature was quickly raised to a predetermined higher value and kept constant up for 1000 s, during which the intensity of emission released from the sample was measured and recorded against time.

The STPs were measured at selected temperatures in the range of 35–600 K using a set-up based on a closed-cycle He cooler with a 'hot stage' and a temperature controller. The cooler was equipped with a sample chamber designed to accommodate a γ-radioactive source (Cs^{137}). A standard synchronous photon counting method was employed to record time profiles of γ-excited emission pulses.

The VUV experiments (luminescence and excitation spectra, pulsed VUV-excited emission time profiles) were conducted at the SUPERLUMI station of HASYLAB, Hamburg,

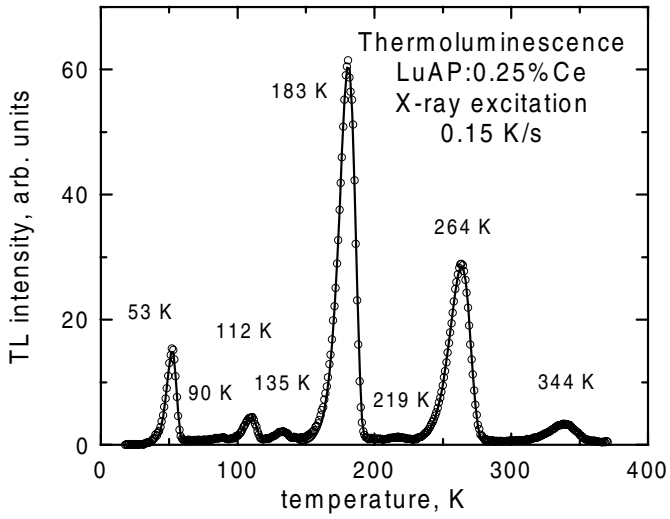

Figure 1. The TL glow curve of LuAP:0.25% Ce following an 18 h x-ray irradiation at 4 K. Empty circles represent experimental points. The heating rate was 9 K min^{-1} and thermal lag, by which all the experimental points were shifted, was assumed to be 3.1 K (see text). The solid line represents a TAMTAM fit. Trap parameters obtained from the fit are summarized in table 1.

Germany. A detailed description of SUPERLUMI's experimental facilities was given by Zimmerer [35] and is also available on line [36].

3. Experimental results

3.1. Low temperature thermoluminescence (ltTL) and isothermal decays (ITDs)

The glow curve of LuAP (0.25% Ce) measured after the x-ray irradiation at a heating rate of 9 K min^{-1} is shown in figure 1. In addition to the 344 K glow peak, two larger and two smaller glow peaks (at 183, 264, 53 and 90 K, respectively) that have been identified and analysed previously [21, 27, 28, 30], the curve shows new glow peaks at 112, 135 and 219 K.

Since under first-order kinetics (note the asymmetric shapes of glow peaks) different traps responsible for different overlapping glow peaks do not interfere, a complex glow curve can be represented as a sum of single-peak terms each given by the Randall–Wilkins formula [29]:

$$I(T) = \sum_{i=1}^{N} n_{0i} s_i \exp\left(-\frac{E_i}{kT}\right) \exp\left(-\frac{s_i}{\beta}\right) \int_{T_0}^{T} \exp\left(-\frac{E_i}{kT}\right) \mathrm{d}T \qquad (1)$$

where N is the number of independent traps, T is the true sample temperature (corrected for thermal lag, which is the difference between the true sample temperature and that of the heating element), β is the heating rate, n_{0i}, s_i and E_i are initial concentrations of occupied traps, frequency factors and trap depths, respectively.

A solid line shown in figure 1 represents a theoretical fit to experimental points obtained by a TAMTAM procedure based on expression (1) and developed by T M Piters. The values of trap parameters (trap depths and frequency factors) retrieved by this procedure depend on the assumed value of thermal lag as shown in figure 2. We find that for the lag value of about 3.1 K, the values of trap parameters obtained by the TAMTAM procedure for the 53 K glow curve are reasonably close to those derived from the ITD experiments in the vicinity of the

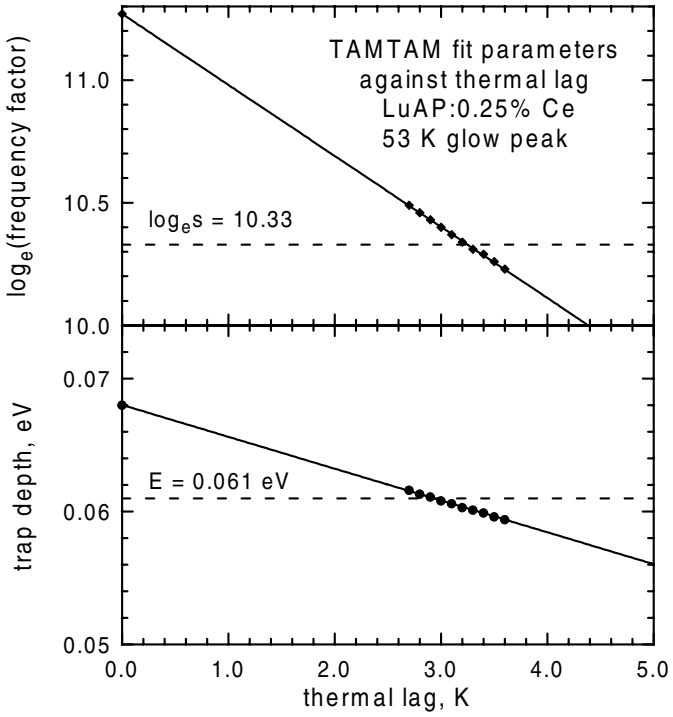

Figure 2. TAMTAM fit parameters (energy depth, E and natural logarithm of frequency factor, ln s) against a variable thermal lag for the 53 K glow peak of LuAP:0.25% Ce. (filled circles and diamonds) we by points show values obtained by the TAMTAM procedure applied to a 53 K glow peak that has been shifted by a given value of thermal lag. Solid lines are straight line fits to circles and diamonds. Dashed horizontal lines correspond to trap parameter values derived from the ITD fits (0.61 eV and 10.33, see figures 3 and 4 and text). Intercept values suggest that the true thermal lag is about 3.1 K.

Table 1. Trap parameters derived from the glow curve fitting by the TAMTAM procedure for LuAP:0.2% Ce. The heating rate was 0.15 K s^{-1}. The 53 K glow peak has been fitted separately. Thermal lag was assumed to be 3.1 K (see text).

Peak number i	Glow peak T_0 (K)	n_{0i}/n_{05}	E_i (eV)	ln s_i
1	53	–	0.0606	10.37
2	90	0.0152	0.065	4.59
3	112	0.0488	0.230	21.07
4	135	0.0334	0.185	12.13
5	183	1.00	0.490	27.90
6	219	0.020	0.390	16.89
7	264	0.595	0.814	32.23
8	344	0.0837	0.947	28.56

same glow peak. The ITD experiments including the results obtained for the 53 K glow peak will be discussed shortly. The TAMTAM fit parameters for all the glow peaks shown in figure 1 assuming a 3.1 K thermal lag are summarized in table 1.

It is interesting to note that the intensities and ordering of the eight glow peaks shown in figure 1 might suggest that the eight traps corresponding to these glow peaks fall into

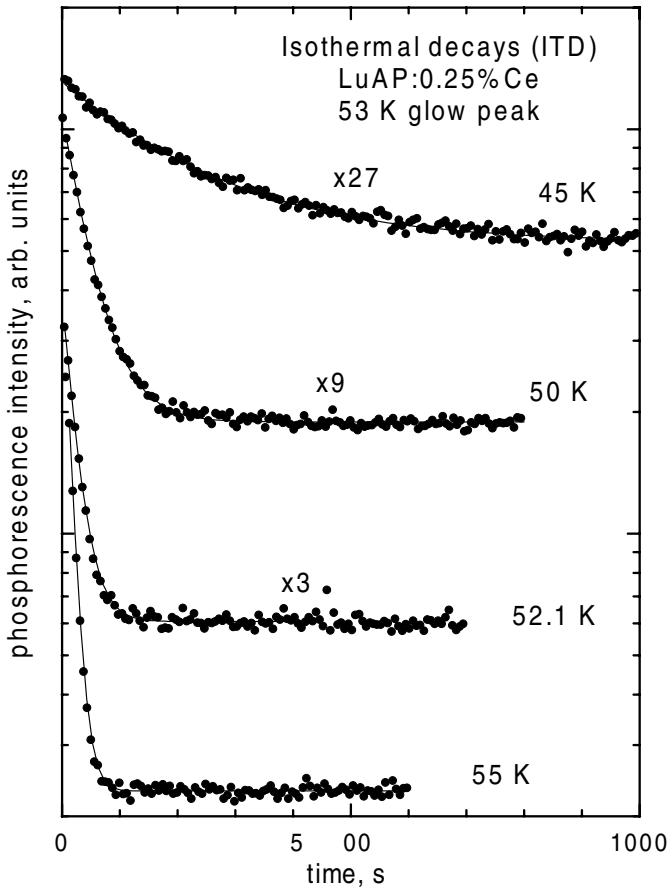

Figure 3. Representative ITD curves of LuAP:0.25% Ce measured in the vicinity of the 53 K glow peak at selected temperatures indicated in the figure. Solid circles represent experimental points and solid lines depict one-exponential fits with additional fitting constant to correct for the background. The curves have been shifted vertically for clarity of presentation.

two distinct groupings. Each grouping starts with the shallowest dominant 'leading' trap (53 and 183 K) followed by one minor trap (90 and 219 K) and two major traps of diminishing intensities (112 and 135 K in the first grouping and 264 and 344 K in the second grouping). We will demonstrate later that the dominant trap of those identified earlier (1.74 eV, the glow peak of 510 K at 1 K s^{-1} heating rate) by Wojtowicz *et al* [25] might be related to 53, 135, 183 and 264 K traps and might represent, therefore, the leading trap of the third grouping.

In figure 3 we present by experimental points a set of representative phosphorescence ITDs measured in the vicinity of the 53 K glow peak (at 45, 50, 52.1 and 55 K) of LuAP:0.25% Ce. A reasonably good fit to experimental points was obtained using a one-exponential expression with a background, denoted by thin solid lines. Time constants derived from these fits were 221.4, 44.7, 22.9 and 12.8 s, respectively. As expected, the decay constant of the ITD curve shortens as temperature increases.

Assuming that ITD decays are due to radiative recombination that follows thermally activated release of electrons from traps, the ITD decay times simply reflect the trap lifetimes

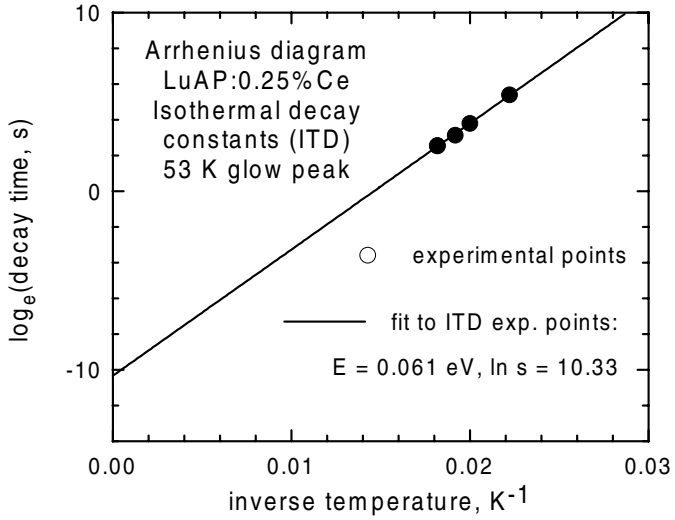

Figure 4. Arrhenius plot of natural logarithm of ITD decay constants against inverse temperature in the vicinity of the 53 K glow peak. The slope and intercept of the straight line fitted to experimental points (filled circles) yield the activation energy (E, trap depth) and frequency factor (ln s).

at the predetermined constant temperatures. The trap lifetime (or the trap emission rate, p) can be expressed in the Arrhenius form

$$p = \frac{1}{\tau} = s \exp\left(-\frac{E}{kT}\right) \tag{2}$$

where s and E are the frequency factor and activation energy (trap depth), respectively. Taking the natural logarithm of both sides of this equation gives the following formula:

$$\ln \tau = \frac{E}{k}\frac{1}{T} - \ln s \tag{3}$$

that can be conveniently used to extract the trap parameters s and E by plotting the natural logarithm of ITD decay time constants against inverse temperature, T^{-1}. Such a plot for a 53 K trap is shown in figure 4. Experimental points (decay times from fits) are denoted by filled circles and a straight line fit to these points is represented by a solid line. The trap parameter values derived from the fit are 0.061 eV (E) and 10.33 (ln s). The intercept of horizontal straight lines corresponding to these values with straight line fits to experimental points in figure 2 was used to evaluate the true thermal lag value as 3.1 K. The trap parameters derived from the TAMTAM fit for this particular thermal lag value are 0.0606 eV (E) and 10.37 (ln s).

The agreement between parameters found from TL fits and those found from ITD fits is not always as good as in the case of the 53 K glow peak. In figure 5 we present by experimental points (filled circles) the set of ITD decay times measured by the same procedure for a number of temperature points in the vicinity of the major glow peak at 183 K. The dashed line presents a straight line fit to experimental points that provides one set of trap parameters (0.438 eV and 24.25). The second straight line shown as a solid line was calculated using a different set of trap parameters found from the TAMTAM fit (0.490 eV, 27.90). Although the lines converge at temperatures in the vicinity of the glow peak (as expected), the difference between the lines for higher temperatures becomes significant. In particular at room temperature (297 K) the trap lifetime calculated from the two sets of parameters would be 777 μs (ITD fit parameters) and 154 μs (ltTL fit parameters).

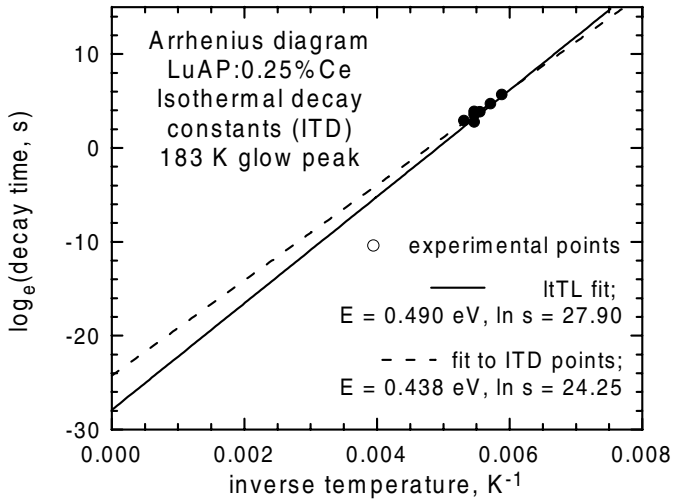

Figure 5. Arrhenius plot of natural logarithm of ITD decay constants against inverse temperature in the vicinity of the 183 K glow peak. The dashed line represents a straight line fit to experimental points denoted by filled circles. The solid line was calculated using trap parameters obtained from the ltTL glow curve fitting by the TAMTAM procedure.

The ITD experiments have been extended to include all the observed glow peaks shown in figure 1. The decay times found from fits of experimental decays to a one-exponential expression with an additional constant to account for a background using the same procedure as in the case of the 53 and 183 K glow peaks are denoted by filled circles in figure 6. Thin solid straight lines represent fits to experimental points. The points obtained for the weakest glow peaks at 90 (one point) and 219 K (two points) have not been fitted. The ITD fit parameters are summarized in table 2. Note that while the trap energies found from the slope values of the straight line fits are reasonable, the frequency factor values are much less reliable (to find an intercept, a significant extrapolation of the straight line to $1/T = 0$ is required). The STP measurements that provided the STP points denoted by filled diamonds in figure 6 will be discussed shortly. With the exception of decay times from the STPs measured at elevated temperatures (350, 420 and 580 K) that were included in the fit denoted by a thin broken line, these points have not been included in fits in this figure.

3.2. Scintillation time profiles (STPs)

If the scintillation light production mechanism is due to radiative recombination that follows thermally activated release of electrons from traps [25], then STPs measured at different temperatures should include components decaying with time constants that correspond to trap lifetimes at these predetermined temperatures according to formulae (2) and (3). Therefore STP experiments are likely to provide additional points for Arrhenius plots shown in figure 6 and, since they are expected to fall into different ranges of decay times (tens and hundreds of nanoseconds instead of tens and hundreds of seconds), should improve the quality of fits leading to trap parameters.

In figure 7 we show STPs measured under gamma excitation as described earlier, at selected temperatures between 35 and 600 K. Experimental traces are denoted by jagged thin lines and three-exponential fits are represented by solid lines. Note that some of these traces (at 296 and 580 K) show lesser contribution while others (at 180 and 350 K) show greater

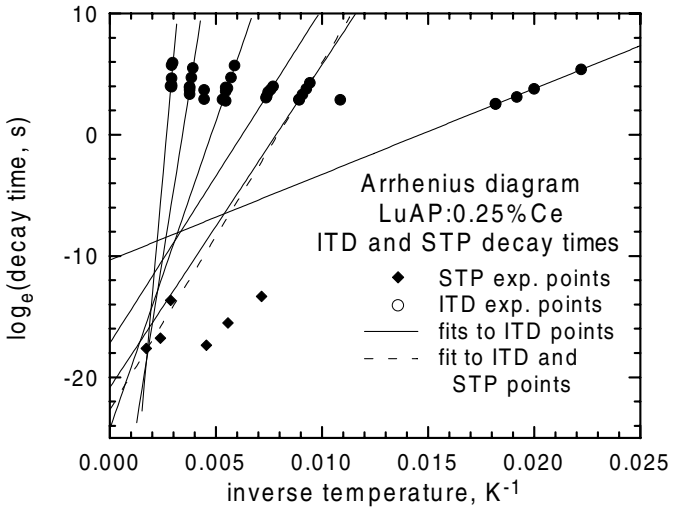

Figure 6. Arrhenius plot of natural logarithm of ITD and STP decay constants against the inverse temperature. ITD experimental points, denoted by filled circles, have been measured for all the glow peaks identified in figure 1. STP experimental points are denoted by filled diamonds. Thin solid lines depict straight line fits to ITD experimental points; the STP experimental points have not been included in these fits. The ITD points obtained for the weakest glow peaks at 90 and 219 K have not been fitted. A thin broken line represents the fit to ITD points obtained in the vicinity of the 112 K glow peak and STP points obtained at elevated temperatures (350, 420 and 580 K). A summary of the fit parameters is given in table 2.

Table 2. Trap parameters derived from the straight line fits to ITD time constants for LuAP:0.25% Ce. The second set of parameters for the 112 K glow peak was obtained from the straight line fit to ITD points and three points derived from the scintillation time profiles at elevated temperatures (350, 420 and 580 K).

Peak number i	Glow peak T_0 (K)	E_i (eV)	ln s_i
1	53	0.061	10.33
2	90	–	–
3	112	0.230	20.84
3 (ITD and STP)	112	0.247	22.67
4	135	0.238	17.18
5	183	0.438	24.25
6	219	–	–
7	264	0.947	37.52
8	344	1.69	52.21

contribution due to slower components. The parameters of fits obtained for all the measured time profiles are summarized in table 3. The contributions of each of the three components were calculated by taking the product of the time constant and the zero-time amplitude obtained from fits and are given in the table as percentage fractions of the total (with no background included).

Although no systematic trend is apparent from the superficial inspection of the table, we have selected some components that have decay times longer than the radiative lifetime of the Ce^{3+} ion in LuAP (18–19 ns) and that show unusually large contributions to time profiles: (140 K, 1.6 μs, 44%), (180 K, 180 ns, 45%), (220 K, 28.7 ns, 78%), (350 K, 1.17 μs, 39%),

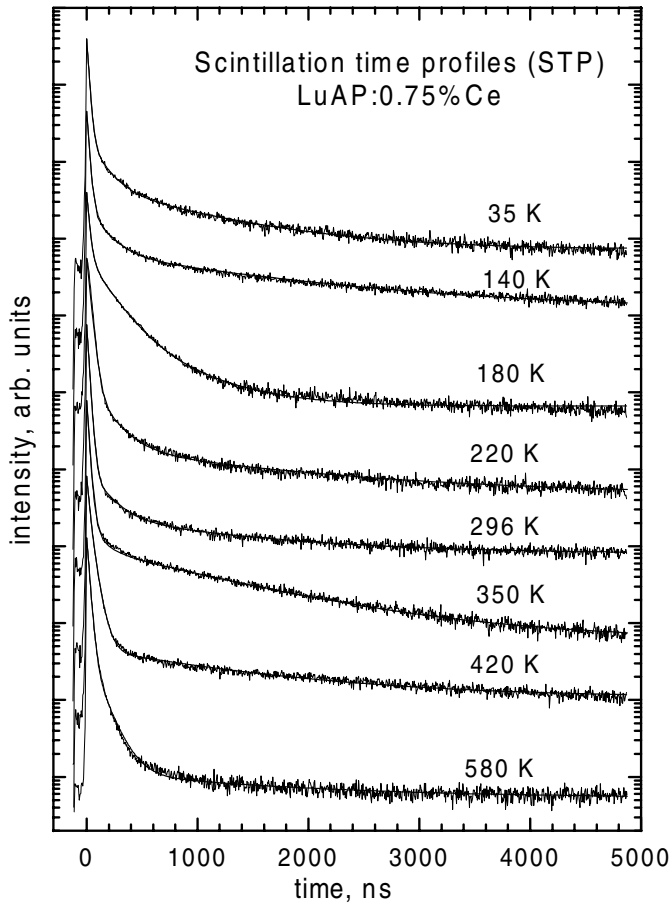

Figure 7. Scintillation time profiles of LuAP:0.75% Ce measured under *gamma* excitation at selected temperatures indicated in the figure. The consecutive curves have been shifted vertically to aid presentation. The jagged thin solid lines represent experimental traces while the thick solid lines depict three-exponential fits with an additional fitting constant to correct for background. Fit parameters are summarized in table 3.

(420 K, 52 ns, 41%) and (580 K, 22.4 ns, 83%). Decay times of these components have been plotted against the inverse temperature in figure 6 (filled diamonds). Note that the diamonds clearly separate into two different sets of points that can probably be assigned to two different traps (or sets of traps). The first trap may be the one that glows at 112 K (350, 420 and 580 K points) although the contribution of traps that produce more prominent glow peaks at higher temperatures (e.g. 183 K) cannot be excluded. The second trap is, most likely, the one that glows at 90 K (140, 180, and 220 K points).

3.3. VUV spectroscopy

The obvious advantage of using the wavelength-resolved VUV excitation is in its potential ability to differentiate between different channels of energy transfer from the host to the activating ion. This enables the study of energy transfer processes that are of key importance for performance of any scintillator material. Although a preliminary report on VUV studies

Table 3. Summary of scintillation time profile measurements for LuAP:0.75% Ce under *gamma* excitation at different temperatures. Decay times and percentage contributions represent parameters derived from three-exponential fits with an additional constant (not included) to account for background.

	Component I		Component II		Component II	
Temperature	Decay time (ns)	Contribution (%)	Decay time (ns)	Contribution (%)	Decay time (ns)	Contribution (%)
35	19.2	54	137	16	970	30
140	18.9	40	155	16	1630	44
180	21.9	36	180	45	530	19
220	28.7	78	170	10	1650	12
296	18.9	80	160	8	1300	12
350	19.5	56	103	5	1170	39
420	22.8	43	52	41	1350	16
580	22.4	83	114	14	1560	3

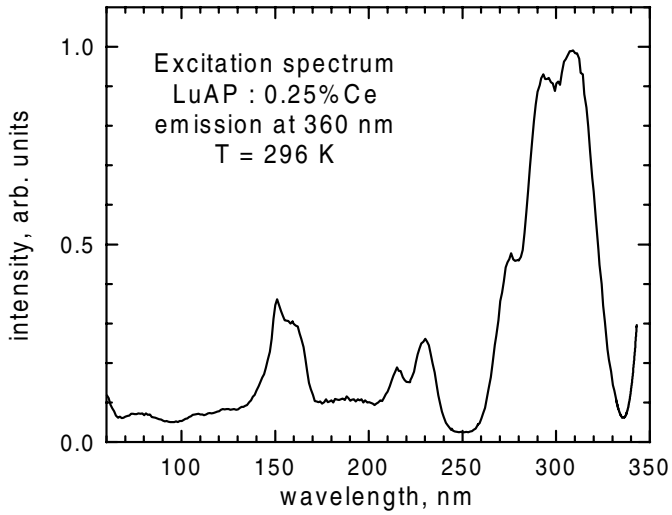

Figure 8. Excitation spectrum of the Ce emission at 360 nm in LuAP:0.25% Ce at 296 K. The spectrum was corrected using the salicylate standard. Note that the wavelength resolved five 4f–5d bands between 200 and 330 nm, a broad 4f–6s band at 190 nm and a double peaked 'host band' at about 150 nm. The intense 'VUV response' of LuAP is consistent with its good scintillation efficiency.

performed by us at the Superlumi station of Hasylab [35, 36] on LuAP has already been published [32], no full account of this work has been given as yet.

In figure 8 we present the excitation spectrum of the characteristic Ce^{3+} 5d–4f emission in LuAP at 360 nm. In addition to the well known Ce^{3+} 4f–5d and 4f–6s bands, the spectrum reveals a shorter wavelength double peak band in the vicinity of the bandgap energy at about 150 nm superimposed on a long, almost featureless, tail extending far into the VUV. These so-called 'host' band and relatively high 'VUV response' have previously been associated with occurrence of energy transfer mechanisms that enable the material to scintillate efficiently [16, 17, 22]. Although the shorter wavelength side of the host band is likely to be severely distorted by strong variations of LuAP reflectivity at these wavelengths (see e.g. [37]), we

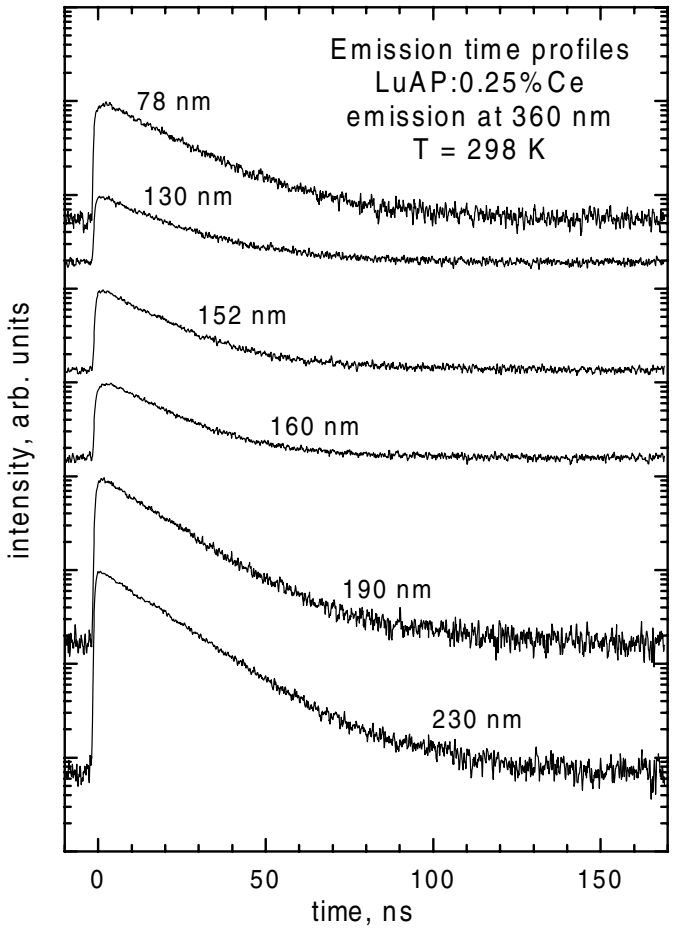

Figure 9. Emission time profiles of LuAP:0.25% Ce under excitation by synchrotron pulses of different UV and VUV wavelengths at room temperature (298 K). The emission wavelength was set at 360 nm. The consecutive traces have been shifted vertically to aid presentation.

can assume that excitonic transitions are more likely to contribute to the longer wavelength side of this band. As the excitation wavelength gets shorter, the electrons and holes generated by a VUV photon have more kinetic energy and are more likely to separate. This explains differences in excitation spectra of Ce and host emissions that were observed previously [16, 17].

Excitonic and free-electron–hole-pair effects are probably responsible for large variations of emission time profiles (the emission wavelength was set at 360 nm) shown in figure 9. These profiles were excited at 298 K by pulsed (below 0.5 ns duration) synchrotron irradiation at different wavelengths, as indicated in the figure. We observe that direct excitations into any of the Ce^{3+} ion, 4f–5d (e.g. at 230 nm) or 4f–6s (190 nm), absorption bands produce nearly single-exponential decays of about 17–18 ns time constants and very short rise times, most likely reflecting the instrumental response function (including the synchrotron pulse width). In contrast, all profiles obtained from excitations at shorter wavelengths contain components that are significantly slower, and display some longer finite rise times.

It has been pointed out that in addition to slow scintillation components (afterglow), very shallow, short-lived traps can also modify the rising part of the scintillation time profile [25]. In the system consisting of one recombination centre and one trap and evolving under first-order kinetics, the scintillation time profile that follows an instantaneous *gamma* excitation is described by the following expression [25]:

$$I(t) = \frac{n_{\mathrm{Ce},0}}{\tau_{\mathrm{rad}}} \exp\left(-\frac{t}{\tau_{\mathrm{rad}}}\right) + \frac{n_0}{\tau - \tau_{\mathrm{rad}}}\left[\exp\left(-\frac{t}{\tau}\right) - \exp\left(-\frac{t}{\tau_{\mathrm{rad}}}\right)\right] \tag{4}$$

where $n_{\mathrm{Ce},0}$ and n_0 are the initial concentrations of excited Ce^{3+} ions and trapped electrons, respectively, τ_{rad} is the Ce^{3+} radiative lifetime and τ is the trap lifetime given by expression (2). In this formula the two terms, describing the 'direct' (or 'prompt') and 'delayed' components of scintillation pulse, are determined by initial concentrations $n_{\mathrm{Ce},0}$ and n_0 that also fix the contributions of the two recombination channels, direct and trap-mediated recombinations via Ce^{3+} ions. Note that for trap lifetime τ shorter than radiative lifetime τ_{rad}, the two exponential terms in the 'trap-mediated' component of the time profile (4) change signs and as a result the decaying part of the profile is described by the radiative lifetime τ_{rad} while the rising part by τ, the trap lifetime.

Consequently the time profiles of Ce emission under short wavelength VUV excitations that are practically equivalent to gamma excitation become particularly interesting since they offer an extension of Arrhenius diagrams (such as the one shown in figure 6) towards even shorter time constants. Therefore such profiles have been measured at temperatures between 10 and 350 K and some of them are presented in figure 10 for the shortest wavelength excitation of 78 nm. Solid lines depict fits to the following two-exponential expression with an additional fitting constant (A_3) to take into account the background and slower scintillation components:

$$I(t) = A_1 \exp\left(-\frac{(t - t_0)}{\tau_{\mathrm{eff}}}\right) - A_2 \exp\left(-\frac{(t - t_0)}{\tau_0}\right) + A_3. \tag{5}$$

The fitting parameters, in addition to A_3, are τ_{eff} and τ_0 (effective decay and rise time constants, respectively), and amplitudes A_1 and A_2. The expression (5) can reasonably be expected to provide a good approximation to the one-trap expression (4) only at temperatures for which the trap lifetime is shorter than the Ce^{3+} radiative lifetime or when the trap lifetime is somewhat (but not too much) longer than the Ce^{3+} radiative lifetime. In the first case we should have an 18–19 ns decay and shorter than 18 ns rise time that should vary with temperature, while in the second case we expect a very short and temperature-independent rise time and effective decay time varying with temperature between, say, 20 and 40 ns [26].

The parameters of fits obtained for all measured time profiles are summarized in table 4. The effective decay and rise times are also denoted by experimental points (filled circles and diamonds) in figure 11. Note that rise times of profiles measured below 240 K assume almost constant and very low value while those measured at and above 240 K increase with the inverse temperature up to 7.1 ns (at 240 K). On the other hand, the effective decay times measured below 240 K are clearly higher than radiative Ce^{3+} lifetime of about 18–19 ns. This behaviour is consistent with a trap having a lifetime of 18–19 ns at temperatures between 240 and 220 K.

Unfortunately a straight line fit to experimental points reflecting the rise times measured between 240 and 350 K and denoted in figure 11 by a solid line yields parameters $E = 0.139$ eV and $\ln s = 25.72$, that do not provide a correct value of the trap lifetime between 240 and 220 K (5 ns at 240 and 10 ns at 220 K). Besides, such a trap would not fit any of the traps we have identified so far by using ltTL and ITD experiments. A likely solution of this apparent contradiction is illustrated in figure 12. We assume here that the trap responsible for the rise times is the same as the one producing the glow peak at 90 K. The straight line fit, denoted in figure 12 by a solid line, includes not only the appropriate rise time points (filled

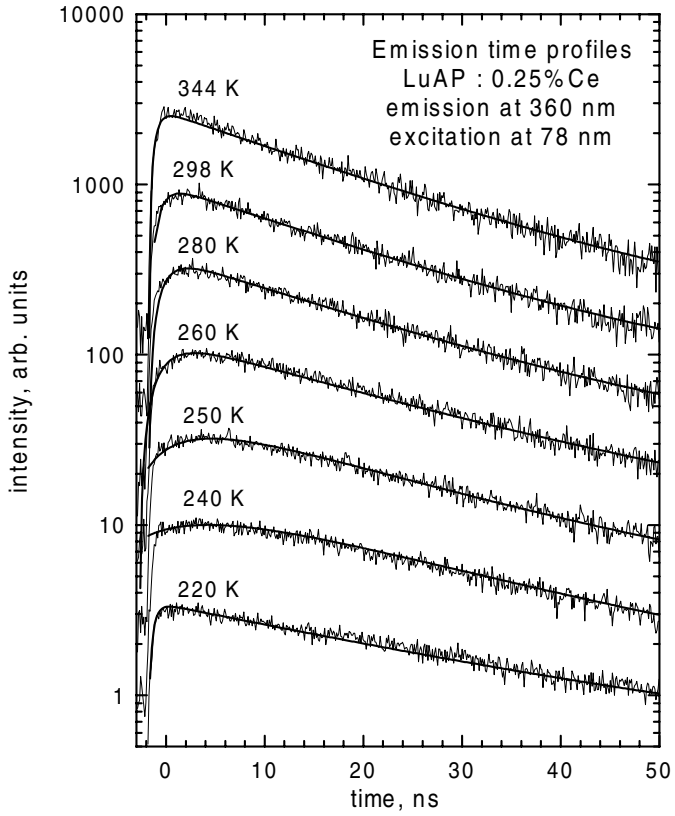

Figure 10. Selection of emission time profiles of LuAP:0.25% Ce under 75 nm excitation by synchrotron pulses at different temperatures indicated in the figure. The emission wavelength was set at 360 nm. The consecutive profiles have been shifted vertically to aid presentation. The jagged thin solid lines represent experimental traces while the thick solid lines depict two-exponential fits with an additional fitting constant to correct for background and longer decay time components (see text). Note the large change of rise time between 220 and 240 K traces. A summary of fit parameters for all measured profiles is given in table 4.

triangles) as in figure 11 but also the 90 K ITD point (filled circle) and appropriate STP points. The parameters obtained from such a fit are $E = 0.262$ eV and $\ln s = 30.73$. Note that at 220 K the lifetime of such a trap is 44 ns (the effective decay at this temperature is 35 ns and the time profile practically shows no rise time), and at 240 K it is 14 ns (the measured rise time is 7.1 ns). Also, such a trap at 235 K would have a lifetime of 18.4 ns, very close to the radiative lifetime of Ce^{3+} ions, as expected from a single-trap model discussed previously. We assume therefore that this fit, not the one denoted by a solid line in figure 11, provides the best evaluation of energy depth and frequency factor of the trap that is responsible for longer rise times at ambient temperatures and the 90 K glow peak in LuAP.

3.4. Scintillation light yield against temperature

Finally in figure 13 we show by experimental points (filled circles) the scintillation LY of LuAP (0.75% Ce) against temperature. In the simplest one-trap model it is assumed that holes generated by the ionizing radiation (a single gamma particle) are instantly captured by the

Table 4. Summary of fit parameters to emission time profiles of LuAP:0.75% Ce measured under VUV excitation of 78 nm at different temperatures. The emission wavelength was set at 360 nm. Effective decay, rise time constants (τ_{eff} and τ_0) and the amplitude ratio (A_2/A_1) represent parameters derived from two-exponential fits with an additional constant (not included) to account for background (see text).

Temperature (K)	Effective decay time, τ_{eff} (ns)	Rise time, τ_0 (ns)	Amplitude ratio (A_2/A_1)
351	19.4	0.6	1.0
344	20.5	0.6	1.0
338	18.9	0.8	0.96
325	20.9	1.0	0.86
314	18.0	1.9	0.69
298	21.2	1.4	0.66
281	23.0	1.9	0.58
270	23.0	2.4	0.79
260	23.2	2.7	1.0
255	26.1	3.1	0.53
250	24.1	4.4	0.60
245	24.1	4.6	0.52
240	25.3	7.1	0.52
220	35.4	0.8	0.50
200	30.8	0.8	1.0
183	26.1	0.7	0.05

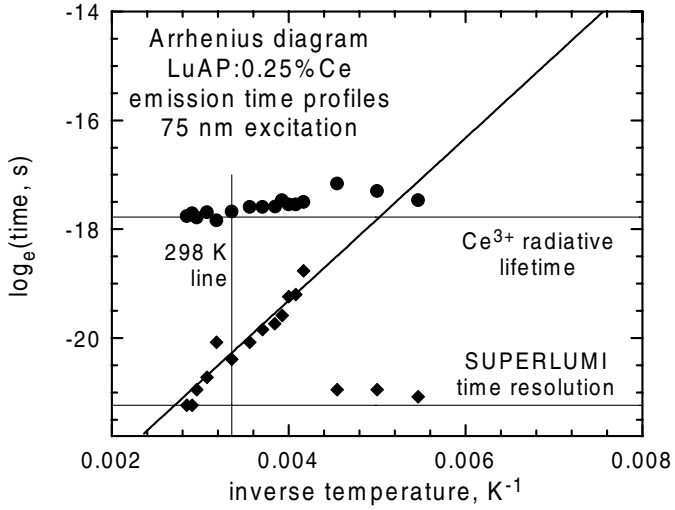

Figure 11. Arrhenius plot of natural logarithm of effective decay and rise time constants (τ_{eff} and τ_0) against inverse temperature. The experimental points, denoted by filled circles (decay constants) and diamonds (rise time constants), have been derived from two-exponential fits shown in figure 10 and summarized in table 4. Note that for temperatures above 240 K the rise time points fall on the sloped straight line pointing to a shallow trap that modifies the rising part of the time profile (see text). Thin horizontal lines correspond to the Ce^{3+} radiative lifetime (19 ns) and the timing resolution of the Superlumi experimental set-up (0.6 ns). A vertical line represents a temperature of 298 K.

Ce^{3+} ions, and electrons are then captured by the Ce^{4+} ions (creating excited Ce^{3+} ions) and electron traps (see e.g. [26]). Then the formula describing the scintillation LY dependence on

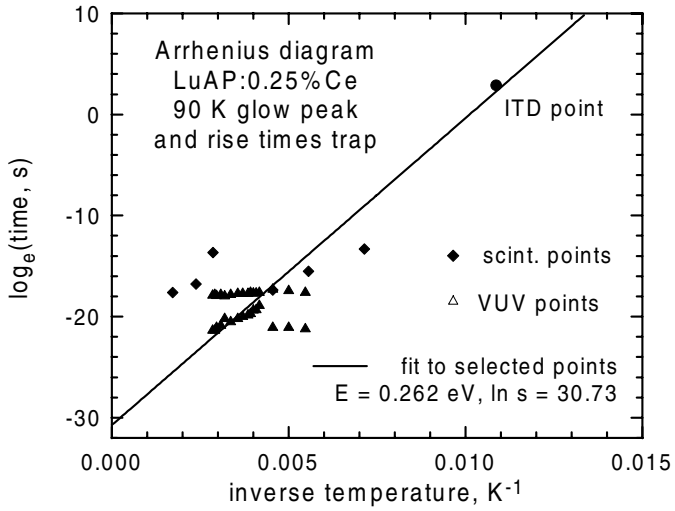

Figure 12. Arrhenius plot of natural logarithm of time constants against inverse temperature. The experimental points, denoted by triangles, represent effective decay and rise time constants obtained from the VUV excited time profiles in table 4. The experimental points denoted by filled diamonds were derived from fits to scintillation time profiles summarized in table 3. The filled circle represents an ITD point obtained from the fit to ITD measured at the 90 K glow peak. The solid line depicts a straight line fit to selected experimental points (see text).

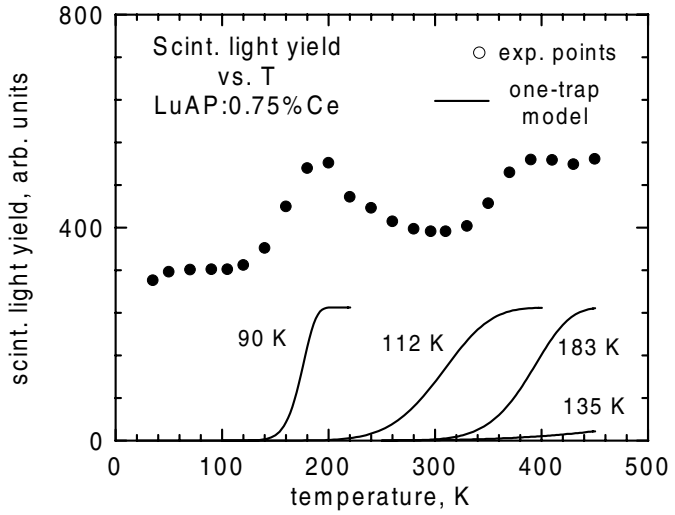

Figure 13. The scintillation LY of LuAP:0.75% Ce against temperature. Experimental points are denoted by filled circles (0.5 μs shaping time). The solid line represents a one-trap model simulation (see text) for consecutive traps labelled by the appropriate glow peak temperature.

temperature assumes a form [26]

$$\mathrm{LY} = \mathrm{LY}_0 \left\{ a + b \frac{p\tau_{\mathrm{rad}}}{p\tau_{\mathrm{rad}} - 1} \left[1 + \frac{1}{p\tau_{\mathrm{rad}}} \left[\exp(-2.35\tau_{\mathrm{sh}} p) - 1 \right] \right] \right\} \tag{6}$$

Table 5. Summary of trap parameters (energy depths E_i and frequency factors s_i) for LuAP obtained from TL, ITD, STP and VUV experiments.

Glow peak T_0 (K)	Experiment	E_i (eV)	ln s_i	RT lifetime (298 K)
53	ltTL and ITD	0.0606	10.37	330 μs
90	STP, VUV and ITD	0.262	30.73	1.2 ns
112	STP and ITD	0.247	22.67	2.1 μs
135	ITD	0.238	17.18	360 μs
183	ltTL	0.490	27.90	140 μs
219	ltTL	0.390	16.89	180 ms
264	ltTL	0.814	32.23	560 ms
344	ltTL	0.947	28.56	3900 s
510	TL	1.74	37.5	1.3×10^{13} s

where LY_0 is the maximum possible LY (no traps, all electrons go to Ce^{4+} ions), the branching coefficients a and b describe the initial distribution of electrons between the Ce^{4+} ions ('direct' component) and electron traps ('trap-mediated' component) respectively, p is the trap emission rate (see formula (2)) and τ_{sh} is the shaping time.

Although the LY–T experiments have been previously used to deduce the trap parameters in LuAP by fitting the calculated curve to experimental points [25, 26, 33], here we demonstrate only that traps (parameters of which have already been established in various other experiments) are indeed responsible for the observed thermally induced variations in the LY. Therefore in figure 13 we denote, by solid lines, the theoretical curves calculated using the one-trap formula (6) where we assumed $a = 0$ (no direct component) and $b \neq 0$ to show thermally induced contributions of various traps. Clearly the steps in the experimental LY–T curve are due to the 90, 112 and, probably, also 183 K traps. All other traps, including the 53 K trap, contribute at much higher temperatures, and at room temperature they are responsible for loss of the scintillation light but do not play an active role in the scintillation process.

4. Summary, discussion and conclusions

The various experiments performed on LuAP and reported in this paper, such as TL, ITDs, pulsed VUV and γ-excited luminescence time profiles at various temperatures, unanimously point to electron traps as being responsible for the scintillation performance of this material. The summary of trap parameters found from all these experiments is given in table 5.

We have identified nine traps and established that a shallow trap glowing at about 90 K contributes to the relatively long scintillation rise time of LuAP at room temperature since its lifetime at 298 K is only 1.2 ns. Other traps glowing at 112, 135 and 183 K must contribute to slower scintillation components since their lifetimes at 298 K are 2.1, 360 and 140 μs, respectively. Surprisingly the shallowest identified trap (energy depth of 0.061 eV), that glows at 53 K, is also characterized by a relatively long lifetime of 330 μs due to its very low frequency factor of 3×10^4 s^{-1}. We demonstrated that some of these traps are responsible for large variations of scintillation LY with temperature as reported earlier. All these traps, including two traps glowing at 219 and 264 K that at 298 K have lifetimes of about 0.18 and 0.56 s, respectively, are also responsible for significant differences between the time-gated scintillation LY and a steady-state radioluminescence LY reported in the literature. Finally, the lifetime of a deep trap glowing at 344 K was found to be about 3900 s at 298 K. This trap as well as an even deeper trap identified earlier (glowing at 510 K, with lifetime of about

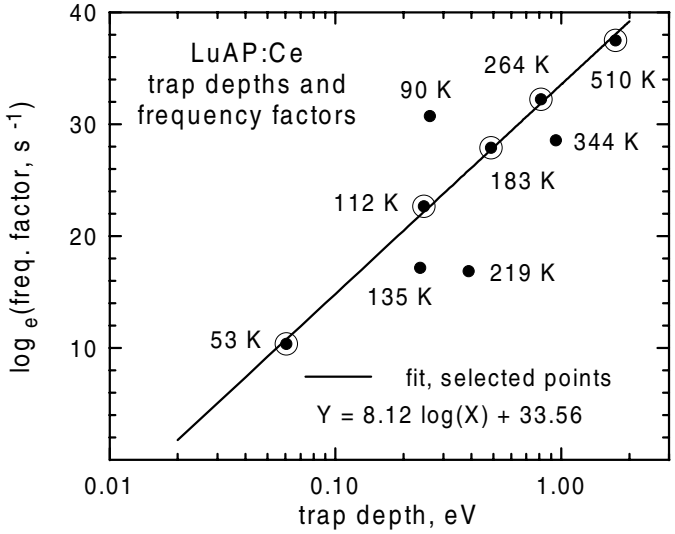

Figure 14. Relationship between trap depths and frequency factors. Points denoted by filled circles correspond to pairs of values characterizing traps labelled by the glow peak temperature. The solid line depicts a straight line fit to selected points (larger empty circles). For discussion see text.

1.3×10^{13} s at 298 K) are also responsible for a scintillation light loss in LuAP at ambient temperatures.

Since for the first time a set of reasonably reliable parameters characterizing a number of traps in LuAP is available, it is tempting to look into possible correlations between them. In figure 14 we show frequency factors and energy depths of all the nine traps plotted in the same diagram using the log x and y scales. Each point in this diagram corresponds to one trap (labelled by the glow peak temperature) and is fixed by the values of parameters (frequency factor and energy depth) of this particular trap. We note that the points corresponding to five different traps (53, 112, 183, 264 and 510 K, denoted by smaller filled circles placed inside *empty* larger circles) lie on one straight solid line indicating that there is a specific relation between these parameters. We also note that four of these traps belong to two different groupings of glow peaks, 53 and 112 K, and 183 and 264 K. The third member of each grouping, labelled 135 and 344 K, lies below the straight line. The minor traps that produce glow peaks at 90 and 219 K close to the glow peaks due to 'leading' traps at 53 and 183 K do not appear to follow any particular pattern.

These observations strongly suggest that at least some of the traps in LuAP are related to a series of common origin native defects or uncontrolled impurities. Although there is no comprehensive study of native defects in LuAP, there are a number of experimental [38] and theoretical [39] studies aimed at defects in the closely related isostructural Y-perovskite, $YAlO_3$ (YAP).

Baryshevsky *et al* [38] point to Schottky type defects (oxygen and cation vacancies) as responsible for a number of absorption and emission bands present in undoped and Ce-doped YAP crystals. However, since the optical transitions assigned to various centres originating from these defects suggest that the corresponding energy levels lie deep in the forbidden energy gap, it is highly unlikely that these centres are able to act as the relatively shallow traps studied in this paper.

On the other hand, Kuklja [39] suggests that since defect formation energies of both Schottky and Frenkel type defects are much higher, the antisite defects (Y_{Al} and Al_Y) are most likely to dominate in YAP and YAG crystals. We note that actually only one of these defects is likely to provide an empty shallow level below the conduction band and the electron capture cross section would be small (no Coulomb attraction). Moreover, since these defects hardly aggregate (no charge), there is no obvious way to obtain a series of relatively shallow levels as observed experimentally.

We conclude that neither Schottky nor antisite disorder is likely to provide a series of native defects that would act as the relatively shallow traps observed experimentally. We note, however, that although Frenkel disorder reaction enthalpies are among the highest, the interstitial cations in YAP and YAG (Al, Y) are the only native defects that have large and negative defect formation energies [39]. We also note that the Y (or Lu in LuAP) atom, placed at the interstitial site, is likely to provide a series of three levels of varying depths corresponding to transitions between the three consecutive charge states of Lu (Lu^0/Lu^{1+}, Lu^{1+}/Lu^{2+}, Lu^{2+}/Lu^{3+}). The Coulomb interaction term resulting from association of Lu with some other charged defect (such as the Lu vacancy) at various positions might be responsible for further diversification of the observed trap depths. However, the experimental evidence that would definitely support the idea of intersitial Lu associated with some other defect is still lacking.

Acknowledgments

This work was performed in the frame of the Crystal Clear Collaboration (All the authors are members of the Crystal Clear Collaboration). We gratefully acknowledge the financial support provided by the Polish Committee of Scientific Research, KBN (grant no 2P03B04914), the US Department of Energy (grant nos DE-FG-02-90ER61033 and DE-FG02-96-ER82117), the IHP-Contract HPRI-CT-1999-00040 of the European Community and a grant from N Copernicus University. We are also very grateful to Dr M H Randles of Litton-Airtron who grew the crystals of LuAP, Dr T M Piters of Universidad de Sonora, Hermosillo, Mexico who wrote and let us use the TL-fitting procedure TAMTAM, Professor G Zimmerer and Dr M Kirm, who provided all necessary assistance and help in VUV experiments at the Superlumi station of HASYLAB in Hamburg, and our colleagues from the Crystal Clear Collaboration for many fruitful discussions.

References

[1] Adeva B *et al* 1990 *Nucl. Instrum. Methods* A **289** 35
[2] Bloomfield P*et al* 1995 *Phys. Med. Biol.* **40** 1105
Lecomte R *et al* 1996 *IEEE Trans. Nucl. Sci.* **44** 1952
[3] Melcher C L and Schweitzer J S 1992 *IEEE Trans. Nucl. Sci.* **39** 502
[4] Baryshevsky V G, Kondratiev D M, Korzhik M V, Kachanov V A, Minkov B I, Pavlenko V B and Fyodorov A A 1993 *Nucl. Tracks Radiat. Meas.* **22** 11
[5] Minkov B I 1994 *Functional Mater.* **1** 103
[6] Moses W W, Derenzo S E, Fyodorov A, Korzhik M, Gektin A, Minkov B and Aslanov V 1995 *IEEE Trans. Nucl. Sci.* **42** 275
[7] Lempicki A, Randles M H, Wisniewski D, Balcerzyk M, Brecher C and Wojtowicz A J 1994 *IEEE Nuclear Science Symp. and Medical Imaging Conf. Record (Piscataway, NJ, 1995)* ed R C Trendler p 307
Lempicki A, Randles M H, Wisniewski D, Balcerzyk M, Brecher C and Wojtowicz A J 1995 *IEEE Trans. Nucl. Sci.* **42** 280

[8] Moszynski M, Wolski D, Ludziejewski T, Lempicki A, Brecher C, Wisniewski D and Wojtowicz A J 1996 *Proc. Int. Conf. Inorganic Scintillators and Their Applications, Scint'95* ed P Dorenbos and C W E van Eijk (Delft: Delft University Press) p 348
Moszynski M, Wolski D, Ludziejewski T, Kapusta M, Lempicki A, Brecher C, Wisniewski D and Wojtowicz A J 1997 *Nucl. Instrum. Methods* A **385** 123
[9] Mares J A, Nikl M, Chval J, Dafinei I, Lecoq P and Kvapil J 1995 *Chem. Phys. Lett.* **241** 311
[10] Petrosyan A G and Pedrini C 1996 *Proc. Int. Conf. Inorganic Scintillators and Their Applications, Scint'95* ed P Dorenbos and C W E van Eijk (Delft: Delft University Press) p 498
[11] Dujardin C, Pedrini C, Bouttet D, Verweij J W M, Petrosyan A G, Belsky A, Vasil'ev A, Zinin E I and Martin P 1996 *Proc. Int. Conf. Inorganic Scintillators and Their Applications, Scint'95* ed P Dorenbos and C W E van Eijk (Delft: Delft University Press) p 336
[12] Dujardin C, Pedrini C, Meunier-Beillard P, Moine B, Gacon J C and Petrosyan A 1997 *J. Lumin.* **72–74** 759
[13] Dujardin C *et al* 1998 *IEEE Trans. Nucl. Sci.* **45** 467
[14] Dujardin C *et al* 1998 *J. Phys.: Condens. Matter.* **10** 3061
[15] See e.g. Brookhaven and Hasylab annual reports available on line at www.brookhaven.gov and www.hasylab-desy.de
[16] Wojtowicz A J 1996 *Proc. Int. Conf. Inorganic Scintillators and Their Applications, Scint'95* ed P Dorenbos and C W E van Eijk (Delft: Delft University Press) p 95
[17] Wisniewski D, Wojtowicz A J and Lempicki A 1997 *J. Lumin.* **72–74** 789
[18] Pedrini C, Bouttet D, Dujardin C, Belsky A and Vasil'ev A 1996 *Proc. Int. Conf. Inorganic Scintillators and Their Applications, Scint'95* ed P Dorenbos and C W E van Eijk (Delft: Delft University Press) p 103
[19] Wojtowicz A J, Lempicki A, Wisniewski D, Balcerzyk M and Brecher C 1996 *IEEE Trans. Nucl. Sci.* **43** 2168
[20] McKeever S W S 1985 *Thermoluminescence of Solids* (Cambridge: Cambridge University Press)
[21] Drozdowski W, Wisniewski D, Wojtowicz A J, Lempicki A, Dorenbos P, de Haas J T M, van Eijk C W E and Bos A J J 1997 *J. Lumin.* **72–74** 756
[22] Wisniewski D, Drozdowski W, Wojtowicz A J, Lempicki A, Dorenbos P, de Haas J T M, van Eijk C W E and Bos A J J 1996 *Acta Phys. Pol.* A **90** 377
[23] Bartram R H, Hamilton D S, Kappers L A and Lempicki A 1997 *J. Lumin.* **75** 183
[24] Wojtowicz A J, Drozdowski W, Wisniewski D, Wisniewski K, Przegietka K R, Oczkowski H L and Piters T M 1998 *Radiat. Meas.* **29** 323
[25] Wojtowicz A J, Glodo J, Drozdowski W and Przegietka K R 1998 *J. Lumin.* **79** 275
[26] Wojtowicz A J 1999 *Acta Phys. Pol.* A **95** 165
[27] Wisniewski D 1998 *PhD Thesis* N Copernicus University, Torun
[28] Lempicki A and Glodo J 1998 *Nucl. Instrum. Methods* A **416** 333
[29] Randall J T and Wilkins M H F 1945 *Proc. R. Soc.* A **184** 366
[30] Glodo J and Wojtowicz A J 2000 *J. Alloys Compounds* **300–301** 289
[31] Wojtowicz A J, Szupryczynski P, Glodo J, Drozdowski W and Wisniewski D 2000 *J. Phys.: Condens. Matter.* **12** 4097
Glodo J, Szupryczynski P and Wojtowicz A J 1999 *Acta Phys. Pol.* A **95** 259
[32] Wojtowicz A J, Drozdowski W, Glodo J, Szupryczynski P and Wisniewski D 1998 VUV studies of radiative recombination in rare earth activated wide bandgap materials; $LuAlO_3$:Ce *Hasylab Annual Report* available on line at http://www.hasylab-desy.de/science/annual_reports/1998/index.html
[33] Wojtowicz A J, Glodo J, Lempicki A and Brecher C 1998 *J. Phys.: Condens. Matter.* **10** 8401
[34] Lempicki A and Bartram R H 1999 *J. Lumin.* **81** 13
[35] Zimmerer G 1991 *Nucl. Instrum. Methods Phys. Res.* A **308** 178
[36] http://www-hasylab.desy.de/facility/experimental_stations/stations/; see the I-beamline
[37] Tomiki T, Kaminao M, Tanahara Y, Futemma T, Fujisawa M and Fukudome F 1991 *J. Phys. Soc. Japan* **60** 1799
[38] Baryshevsky V G, Korzhik M V, Minkov B I, Smirnova S A, Fyodorov A A, Dorenbos P and van Eijk C W E 1993 *J. Phys.: Condens. Matter.* **5** 7893
[39] Kuklja M M 2000 *J. Phys.: Condens. Matter.* **12** 2953